

## CHARACTERIZATION OF NICKEL OXIDE NANOPARTICLES SYNTHESIZED VIA RAPID MICROWAVE-ASSISTED ROUTE

D. MOHAMMADYANI

*Materials and Energy Research Center (MERC)  
P.O. Box 14155-4777, Tehran, Iran  
d.mohammadyani@gmail.com*

S.A. HOSSEINI

*Materials and Energy Research Center (MERC)  
P.O. Box 14155-4777, Tehran, Iran  
a\_hosseini@alum.sharif.edu*

S.K. SADRNEZHAAD\*

*Department of Materials Science and Engineering, Sharif University of Technology  
P.O. Box 11365-9466, Tehran, Iran  
sadrnezh@sharif.edu*

Nickel oxide (NiO) nano-particles were produced via a rapid microwave-assisted method. Ni(OH)<sub>2</sub> precursor was obtained by slow drop-wise addition of 0.1M sodium hydroxide to 0.1M nickel nitrate. The mixture was vigorously stirred until the pH reached 7.2. The mixture was then irradiated with microwave to deposit Ni(OH)<sub>2</sub> at an intensified precipitation rate. Drying of the precipitate at 320°C resulted in formation of NiO nano-powder. Mean dimension of this powder was ~30nm according to the images analyzed by transmission electron microscope (TEM) and scanning electron microscope (SEM). X-ray diffraction (XRD) patterns revealed well-crystallized/high-purity nanostructures of the synthesized powder. Microwave utilization increased homogeneity and decreased the mean particle size of the produced NiO powder.

*Keywords:* Nickel oxide; microwave-assisted route; nano-powder; characterization.

### 1. Introduction

Nano-particle oxides of transition metals have attracted materials scientists. These materials have exceptional properties which stimulate many advanced applications.<sup>1-3</sup> Nano-structured nickel oxide is a prominent example having a large exciton binding energy and a wide band gap ranging from 3.6 to 4.0eV.<sup>4,5</sup> This p-type semiconductor can

---

\* Corresponding author. Tel: +98 21 66165215.  
Email addresses: [sadrnezh@sharif.edu](mailto:sadrnezh@sharif.edu) and [sadrnezh@yahoo.com](mailto:sadrnezh@yahoo.com)

be used in optical, electronic, catalytic and super-paramagnetic devices like transparent conductor films, gas sensors, alkaline battery cathodes, dye-sensitized solar cells and solid oxide fuel cells (SOFC).<sup>4-11</sup>

Versatile routes such as sol-gel<sup>11,12</sup>, chemical precipitation<sup>4,7</sup> and anodic arc plasma method (AAPM)<sup>8</sup> have been used to produce nano-powder oxide materials. Microwave heating has such advantages as high-efficiency, nanoparticle rapid-formation, narrow crystallite size distribution and agglomeration diminution with respect to the conventional methods.<sup>13</sup>

Microwave-assisted methods apply electromagnetic waves having 0.001 to 1m wavelength to accelerate the chemical reaction of interest. These wavelengths correspond to frequencies between 0.3 to 300GHz. Synthesis via microwave-assisted routes is simple, energy efficient and time saver.<sup>14</sup> Its utilization results in rapid volumetric heating, high selectivity and great product yield.<sup>13</sup> Energy transfer via microwave irradiation is believed to occur either through resonance or relaxation. Crucial parameters of this method are microwave power, exposure time and energy flow-rate.<sup>13</sup>

Production of nickel hydroxide by rapid microwave-assisted chemical reaction, post heating of nickel hydroxide to form nickel oxide and morphological characterization and structural study of the NiO nano-particles produced by TEM, SEM and XRD are discussed meticulously in this paper.

## **2. Experimental Procedure**

### **2.1. Sample preparation**

Microwave-assisted synthesis of NiO nano-powder comprised three stages: (a) formation of Ni(OH)<sub>2</sub> precursor, (b) microwave irradiation of Ni(OH)<sub>2</sub> and (c) heat treatment of Ni(OH)<sub>2</sub> to convert into NiO. The stage (a) was carried out by drop-wise slow addition of 0.1M sodium hydroxide (NaOH) to 0.1M nickel nitrate Ni(NO<sub>3</sub>)<sub>2</sub> while vigorous stirring of the solution continued until the pH reached 7.2. The mixture was then irradiated by microwave (2.45GHz, 900W, SAMSUNG) so long as a dry green powder precipitated.

Simultaneous thermal analysis (STA-DTA/TG Netzsch STA 409) was carried out to determine the Ni(OH)<sub>2</sub> to NiO conversion temperature under air. STA measurement followed then according to the following procedure: (a) holding the material at 30°C for 1min, (b) heating up from 30 to 600°C at temperature rate of 10°C/min and (c) holding the product at 600°C for 10min. After determining the temperature of nickel hydroxide to nickel oxide conversion by thermal analysis, the oven-dried cake was heated up to 320°C for 1h to form dark gray particles. To eliminate the residual byproducts, the powder was washed out and filtered three times with distilled water. Final washing was then accomplished by pure ethanol.

## 2.2. Product characterization

X-ray diffraction (Unisantic XMD300, GmbH) was used for structural study and characterization of the powders before and after heating. Phase purity of the initial powder was investigated by XRD. Morphological study was carried out by scanning electron microscope (Cambridge-S360, 20kV). Transmission electron microscope (LEO 912AB) images assessed the formation of well crystalline NiO nano-particles.

## 3. Results and Discussion

Fig. 1 shows the X-ray diffraction pattern of the green powder formed after microwave irradiation. XRD analysis showed that this substance is a typical  $\alpha$ -type nickel hydroxide powder. All of the diffraction peaks were broad and belonged to  $\text{Ni}(\text{OH})_2 \cdot 6\text{H}_2\text{O}$  (JCPDS card No. 38-0715). Their broadening could be attributed either to their small grain size or micro-structural distortion. Under the present experimental conditions, the extremely small particle-like structure could be mere motivation for a significant broadening of some diffraction peaks in  $\text{Ni}(\text{OH})_2$  XRD patterns. The XRD pattern indicated “saw-tooth” reflections which were typical of two dimensional turbostratic phases having orientationally disordered layers.<sup>15</sup>

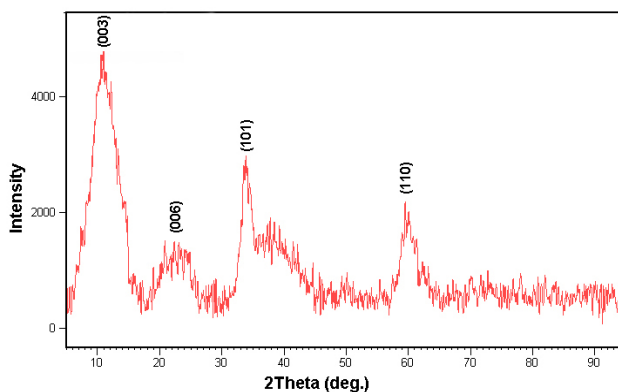


Fig. 1. X-ray pattern of nickel hydroxide powder produced via microwave assisted rout.

$\text{Ni}(\text{OH})_2 \cdot 6\text{H}_2\text{O}$  was produced according to the reaction:



Sodium nitrate was an undesirable byproduct completely soluble in water. It was removed by repeated washing via distilled water.

It was concluded from the STA graphs like the one illustrated in Fig. 2 that two endothermic reactions take place between ambient temperature and 600°C in the sample:





Both reactions accompanied mass reduction due to  $\text{H}_2\text{O}$  removal from the powder. Fig. 2 indicates that these reactions have started at about  $220^\circ\text{C}$  and have finished around  $310^\circ\text{C}$ . In order to suppress any possible unwanted grain growth, a relatively low temperature has been chosen for heat treatment of the sample to form NiO nanoparticles. The oven-dried cake was, therefore, heated at  $320^\circ\text{C}$  for 1h. XRD pattern (Fig. 3) confirmed the formation of nickel oxide by heating the sample (JCPDS card No. 22-1189). No other components were detectable in the final powder.

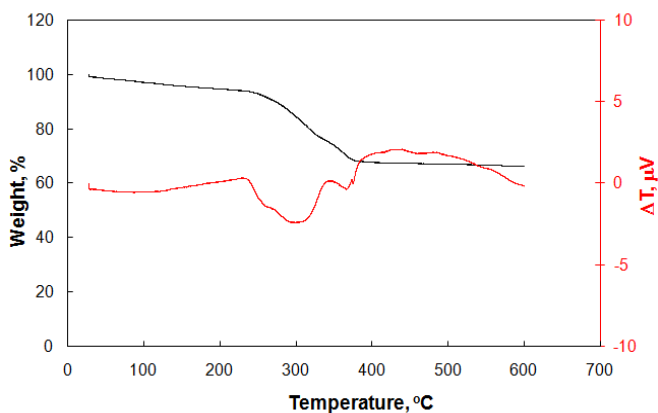


Fig. 2. STA (TG/DTA) graphs of nickel hydroxide. Experimental conditions were: (a) 1min holding at  $30^\circ\text{C}$ , (b)  $10^\circ\text{C}/\text{min}$  temperature raise from 30 to  $600^\circ\text{C}$  and (c) 10min holding at  $600^\circ\text{C}$ .

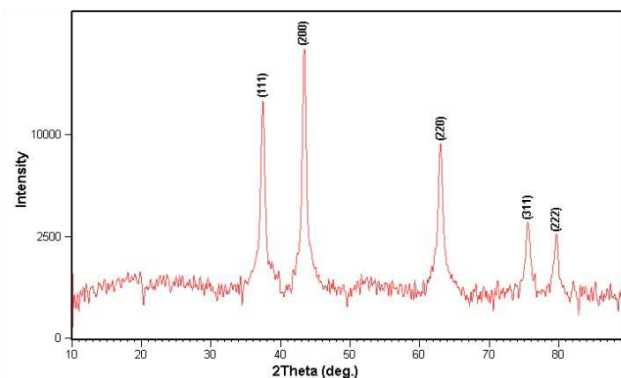


Fig. 3. XRD pattern of the nickel oxide powder produced in this research.

The final product appeared in black color. Green color has commonly been reported for NiO semi-conductor. Color deterioration was attributable to the non-stoichiometric character of the final NiO powder.<sup>16</sup> Fig. 1 shows poor crystallinity of  $\text{Ni(OH)}_2$  precursor. Fig. 3 indicates high crystallinity of NiO nano-powder. According to the Scherer

equation, crystallite size generally decreases with broadening of the longest XRD peak. Table 1 compares the mean crystallite size of the NiO nano-particles produced via microwave-assisted route with the conventional sol-gel method. The mean crystallite size was calculated by application of the Scherer equation:

$$D = \frac{K \lambda}{\beta \cos \theta} \quad (4)$$

$D$  is the mean crystallite size of the powder,  $\lambda=1.54056\text{\AA}$  is the wavelength of Cu  $k_{\alpha}$ ,  $\beta$  is the full width at half-maximum (FWHM) intensity of the (200) peak,  $\theta$  is Bragg's diffraction angle and  $K$  is a constant usually equal to 0.9. The mean crystallite size  $D=19.0\text{nm}$  of the produced NiO powder confirms formation of the nano-crystalline structure. Results indicate that microwave irradiation reduces the mean crystallite size of the synthesized powder.

Table 1. Mean crystallite size of NiO nanoparticles obtained from microwave-assisted and conventional sol-gel routes both evaluated from the Scherer equation.

Procedure	Mean crystallite size (nm)
Conventional sol-gel route	21.8
Microwave-assisted method	19.0

Fig. 5 depicts NiO micrograph of the microwave-assisted powder. Aggregated particles around 50 to 300nm in diameter are observable in the figure. Their creation may be due to the influence of the interfacial energies and interparticle magnetic interactions.

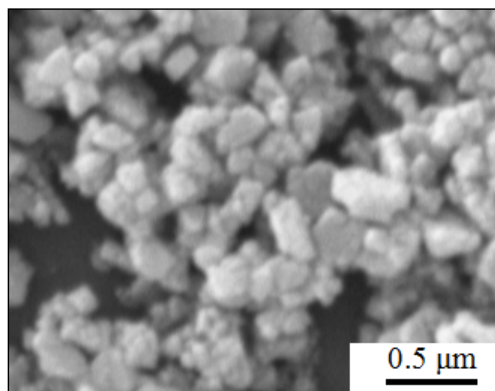


Fig. 5. Micrograph of the nickel oxide nano-powder produced via rapid microwave-assisted route.

TEM images are shown in Fig. 6. They exhibit NiO nano-particles having mean crystallite size of  $\sim 30\text{nm}$ . NaCl-like cubic structure for NiO is assessable from the figure. Slight tilting in the lattice angle can be attributed to the non-stoichiometric composition of the oxide powder produced during the production procedure. Both SEM and TEM

morphologies illustrated in Figs. 5 and 6 indicate that the primary nano-particles are clustered together to form larger agglomerates. The mean aggregate size is ~150nm.

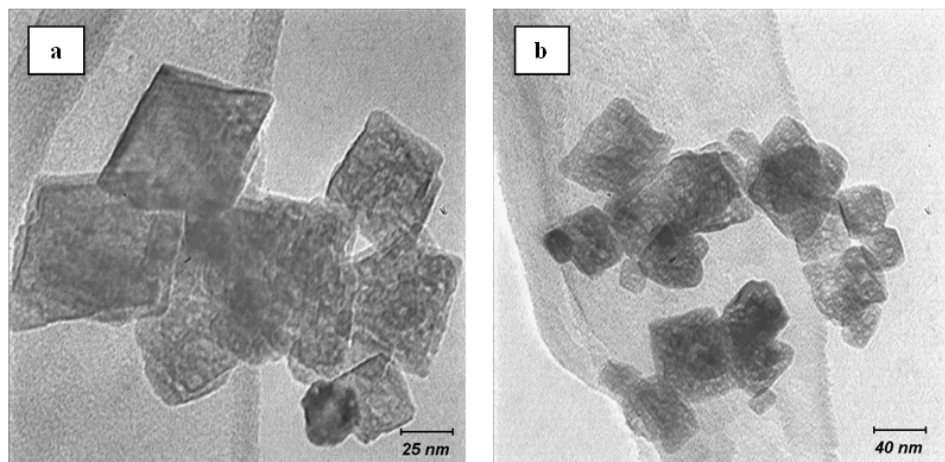


Fig. 6 Transmission electron micrograph of NiO nano-powder synthesized via rapid microwave-assisted route.

One new finding of this research is intensification of the reaction-rate by the microwave-assistance. The Arrhenius law explains the specific rate:

$$k = A \exp (-Q/RT) \quad (5)$$

Where  $k$  is the rate constant,  $A$  is the frequency factor indicating the molecular mobility,  $Q$  is the activation energy,  $R$  is the universal gas constant and  $T$  is the absolute temperature at the reaction interface. According to Eq. (5), there are two ways to increase the rate of a chemical reaction: increasing  $A$  or decreasing  $Q$ . Microwave causes an increase in the molecular vibrations and thus the frequency factor of the reaction increases. Microwave irradiation can also decrease the activation energy  $Q$  of the reaction and thus cause the acceleration. These findings are consistent with those of the previous authors.<sup>17</sup>

#### 4. Conclusion

Highly-crystallized pure nickel-oxide nano-particles with a mean crystallite size of ~30nm were synthesized by a microwave-assisted approach. Morphology of the produced powders showed NaCl-type cubic structure. Microwave irradiation resulted in formation of well-shaped homogeneously crystallized powders. Using microwave irradiation resulted in acceleration of the production rate and reduction of the accomplishment time of the process. Color alteration was recognized during nickel oxide formation. This phenomenon was attributed to the non-stoichiometric character of the nano-particles.

## Acknowledgments

The authors appreciate Iran National Science Foundation for financial support of the research.

## References

1. P. Duran, J. Tartaj, C. Moure, *J. Am. Ceram. Soc.*, Vol. 86 (8), 2003, pp. 1326–1329.
2. J. Wang, L. Gao, *J. Am. Ceram. Soc.*, Vol. 88 (6), 2005, pp. 1637–1639.
3. M. Mazaheri, A.M. Zahedi, M.M. Hejazi, *Mater. Sci. Eng. A*, Vol. 492, 2008, pp. 261–267.
4. J. Bahadur, D. Sen, S. Mazumder, S. Ramanathan, *J. Sol. Sta. Chem.*, Vol. 181, 2008, pp. 1227–1235.
5. H. Sato, T. Minami, S. Takata, T. Yamada, *Thin Solid Films*, Vol. 236, 1993, pp. 27.
6. B.L. Cushing, V.L. Kolesnichenko, C.J. O'Connor, *Chem. Rev.*, Vol. 104, 2004, pp. 3893–3946.
7. Y. Bahari Molla Mahaleh, S.K. Sadrnezhad, and D. Hosseini, *J. Nanomat.*, Vol. 2008, 2008, pp. 1–4.
8. Q. Hongxia, W. Zhiqiang, Y. Hua, Z. Lin, Y. Xiaoyan, *J. Nanomat.*, Vol. 2009, 2009, pp. 1–5.
9. S.A. Needham, G.X. Wang, and H.K. Liu, *J. Power Sources*, Vol. 159 (1), 2006, pp. 254–257.
10. S.S. Kim, K.W. Park, J.H. Yum, Y.E. Sung, *Sol. Energy Mater. Sol. Cells*, Vol. 90, 2006, pp. 283–290.
11. M. Ghosh, K. Biswas, A. Sundaresan, C.N.R. Rao, *J. Mat. Chem.*, Vol. 16, 2006, pp. 106–111.
12. Y. Wu, Y. He, T. Wu, T. Chen, W. Weng, and H. Wan, *Materials Letters*, Vol. 61(14-15), 2007, pp. 3174–3178.
13. T. Krishnakumar, R. Jayaprakash, N. Pinna, V.N. Singh, B.R. Mehta and A.R. Phani, *Materials Letters*, Vol. 63(2), 2009, pp. 242–245.
14. Mirosław Zawadzki, *J. Allo. Com.*, Vol. 451 (1-2), 2008, pp. 297–300.
15. G. Fu, Z. Hu, L. Xie, X. Jin, Y. Xie, Y. Wang, Z. Zhang, Y. Yang, H. Wu, *Int. J. Electrochem. Sci.*, Vol. 4, 2009, pp. 1052–1062.
16. N.N. Greenwood, A. Earnshaw, *Chemistry of the Elements*, Pergamon, Oxford, 1997.
17. P. Lidstrom, J. Tierney, B. Wathey, J. Westman, *Tetrahedron*, Vol. 57, 2001, pp. 9225–9283.